Anal. Methods Environ. Chem. J. 7 (2) (2024) 89-106

AMECJ

Research Article, Issue 2
Analytical Methods in Environmental Chemistry Journal
Journal home page: www.amecj.com/ir

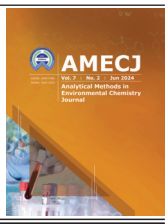

Hydrothermal synthesis of zinc borate as photocatalyst for efficient removal and determination of Congo red dye from aqueous solution by UV-Vis spectroscopy

Hasan Jasim Mohammad [a,*], and Zaki Naser Kadhim [a]
[a] *University of Basra, College of Science, Chemistry Department, Basra, Iraq*

ARTICLE INFO:
Received 26 Jan 2024
Revised form 23 March 2024
Accepted 7 May 2024
Available online 29 Jun 2024

Keywords:
Zinc borate adsorbent
Adsorption
Congo red day
UV-Vis Spectroscopy
Isotherm model

ABSTRACT
This study synthesized zinc borate ($Zn_2BO_3(OH)$, ZB) through one-step precipitation from nano zinc oxide and boric acid. FTIR, XRD, SEM, EDX, and Zeta potential characterized the product. Due to the photocatalyst properties Congo Red Day (CRD) was removed from the aqueous solution. Effective factors on the adsorption efficiency are studied (time, amount of adsorbent, concentration, pH, and temperature). Results of the study indicated that the best amount of adsorbent was obtained at 0.1 g which was used against dye when adsorption capacities equal 6.034 mg g^{-1}. Also, the adsorption capacities [$q_{(mg/g)}$] were obtained at 35.556 mg g^{-1} in the CRD concentration of 50 mg L^{-1}, and [$q_{(mg/g)}$] was equal to 20.154 mg g^{-1} in 100 mL sample at pH 5.5. All adsorption processes using distilled water (DW) were analyzed using UV-Vis spectroscopy. The adsorption capacity was calculated by using Langmuir and Freundlich isotherm models, and results showed that the maximum adsorption capacity (q_{max}) in the Langmuir model was achieved at 212.7 mg g^{-1} for $Zn_2BO_3(OH)$. The R-squared (R^2) or the low coefficient of determination for Langmuir and Freundlich isotherms adsorption were obtained at 0.98 and 0.89, respectively. The kinetic adsorption based on the first-order and second-order pseudo coefficients were achieved at R^2=0.89 and R^2=0.99, respectively. The thermodynamics values (ΔS, ΔG, ΔH) are measured and the results indicate that the adsorption process is spontaneous and endothermic.

1. Introduction

Zinc borates one of the most important materials of the first row in the world [1]. ZB is used for various industries due to their specific properties such as smoke suppressant, synergistic effect, flame retardant, corrosion inhibitors, anti-bacterial properties, good mechanical properties, and high surface area [2]. Colors are among the important chemicals that can be involved in industrial processes in various fields, as they occupy an important commercial place. These colors have multiple sources according to their nature, natural or artificial. The industrial type usually has a dye or pigment source [3]. Substances that work to exclude colors belonging to the dye family are superior to those materials that work to exclude pigment colors because of their high solubility in solvents and do not require additional stages of dispersion. The processes involved in painting fibers and fabrics annually release a lot of harmful waste into river water, causing pollution [4], Where 15 % of the dyes used in industrial painting processes leak into river canals and streams, causing major water

*Corresponding Author: Hasan Jasim Mohammad
Email: Jasiem33@gmail.com
https://doi.org/10.24200/amecj.v7.i02.319

pollution [5]. Therefore, this water must be treated and rid of these chemical pollutants, whether they are dyes or organic or inorganic materials. It is possible that these materials negatively affect the health and safety of humans, threatening the human body with some serious diseases. These risks may be carcinogenic or toxic, and these dyes and chemicals may pose a real danger to the aquatic environment and the living organisms that live in it [6]. Treating and purifying this water from pollutants is neither easy nor simple, as there are many purification theories and many practical principles, as in removal benzene vapor from air by a simple and efficient method based on the triphenyl(3-sulfopropyl)phosphonium *p*-toluene sulfonate as TSIL was coated on multi-walled carbon nanotubes ([TPhPP][SUTO]–MWCNTs) [7], and remove the formaldehyde from the air by a photocatalytic degradation–adsorption process (PC-DAP) by using Bismuth oxide and titanium oxide nanoparticles [8], and toluene removal from air by liquid–gas-phase extraction method by using five ionic liquids were pasted on micro glassy balls [9] , and remove toluene in water and air samples by using new methods based on adsorption, desorption, biodegradation, catalytic process, UV photo irradiation-adsorption, and mixture filtration/adsorption [10], and benzene removal from artificial air after loaded in Robson quartz tubes (RGT) by using A new and efficient method based on solid phase gas extraction (SPGE) with Schiff base immobilized [11], extraction of styrene from water samples by ultra-assisted dispersive cyclic conjugation-micro-solid phase extraction procedure by using (BF_4) [12]. One of the most important applied and practical theories in water purification and filtration is the adsorption process, where the principle of this theory is based on the clinging of molecules of adsorbate substance to molecules of adsorbent substance [13]. This clinging is either based on Van der Waals forces, and thus it is physical adsorption, or based on chemical bonds, and is called chemical adsorption [14]. The two adsorptions used to extract dyes from water are easy to apply, cheap, safe, and harmless to the environment. When dealing with physical adsorption, has some characteristics, including the nature of the forces bonding between molecules of the adsorbate and the adsorbent material, which are weak forces known as Van der Waals forces. Also, this type of adsorption is multi-layered and can be considered a reversible process, as the adsorption process can be reversed by raising the ambient temperature or by changing the conditions of the process, the reverse process of adsorption is called desorption. Chemical adsorption is characterized by the nature of cohesion between adsorbate molecules and adsorbent surface by chemical bonds that are very strong and cannot be separated through certain methods. Therefore, this adsorption is irreversible, this type of adsorption is characterized by its high efficiency in extracting a wide range of impurities and heavy metals from the water to be purified. The dye can be removed from river and lake water by the adsorption process, which is easy and relatively inexpensive and does not cause waste or harm to life in the river environment. It has a relatively large ability to remove pollutants over a wide range and good selectivity, and it can be used at different pollutant concentrations (high or low concentration). What enhances the use of adsorption in removing dyes from water is the diversity and abundance of adsorbent materials of all types, organic, inorganic, and polymeric, especially nano-types, which have a large surface area due to the presence of pores and holes. Activated carbon can be classified as one of the most important types of materials used for the adsorption of dyes from solutions. This is due to its chemical stability, low density, and the soft nature of its composition. Natural or synthetic clay can also be considered a good example of adsorbent material due to its abundance, ease of preparation, and high effectiveness against the molecules desired to be removed from solutions. This is due to its chemical stability, low density, and the soft nature of its composition. Natural or synthetic clay can also be considered a good example of adsorbent material due to its abundance, ease of preparation, and high effectiveness against the

molecules desired to be removed from solutions. Among the dyes that fall within the azo dyes is CR dye which can be considered one of the important colored dyes in many industries, including leather, fiber, paper, and many paint fields (Schema 1). However, the CR dye is toxic and carcinogenic, and this toxicity increases with increasing of the dye concentrations. The surplus of this dye when used, which is usually no less than 15%, as well as poor storage, leaks from factories and textile factories into river streams and lakes, causing pollution of the aquatic environment of the rivers, which leads to harm to living organisms, whether plants, animals, and humans. Leakage of CR dye causes a highly persistent red color to the water that is difficult to set aside [15]. The accumulated concentrations of this dye in living organisms cause health damage, and the most important damage to humans is skin and urinary system problems, liver cirrhosis, and cancer. The study aims to prepare (Zn_2BO_3) and the ability to act as a photocatalyst to remove CRD from an aqueous solution by adsorption method.

2. Material and Methods

2.1. Prepare adsorbent

Zinc borate (Zn_2BO_3) was synthesized by one-single-step precipitation by mixing zinc oxide NP and boric acid with a molar ratio varying from (4:1) in 200 mL of distilled water under a stirrer at 500 rpm at mixing time 10 hours at 60°C, after that the mixture was filtered, then washed for several times with distilled water to remove excess boric acid (Fig.1). The product dried in an oven for 24 hours at 70 C^0 [16].

2.2. Preparing Adsorbate

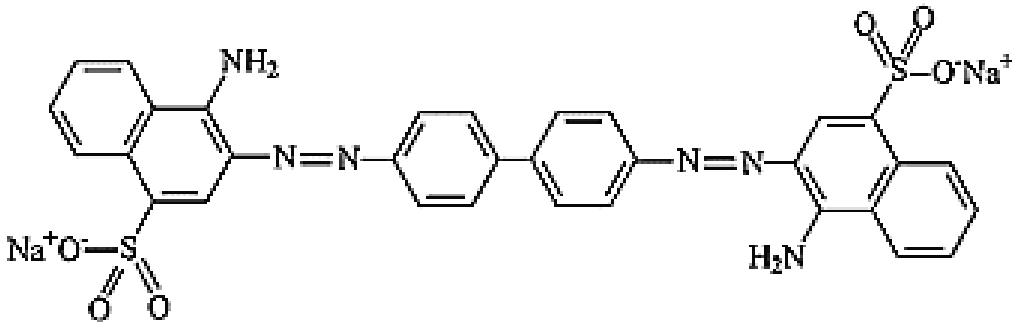

Schema 1. Structure of Congo red dye

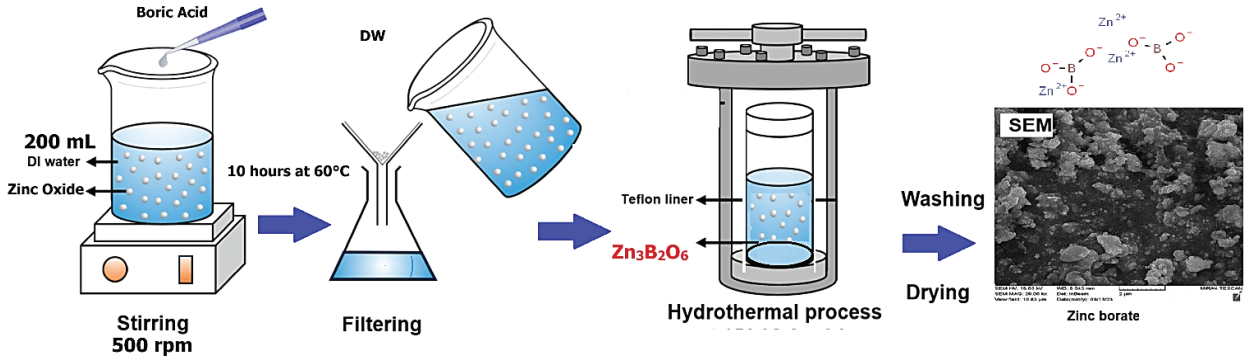

Fig.1. Synthesis of zinc borate (ZB, Zn_2BO_3) by mixing zinc oxide and boric acid

Congo Red dye solution was prepared by dissolving 1.0 g of dye in 1000 mL of distilled water, after that different concentrations of dye were prepared.

2.3. Photocatalyst Procedure

The different dye concentrations were prepared by dissolving solid CR dye at pH 5.5 of 100 mL volume and at the required temperature and placing it in a test tube. After that, an adsorbent (Zn_2BO_3) loaded with a weight of 0.1 g was placed in a shaker and exposed to sunlight for some time, then transported to a centrifuge device to be centrifuged to separate the aqueous solution, which contained the remaining concentration of CR dye that did not adsorb on the adsorbent surface. After that, carefully set aside the solution with a pipette and transfer it to glass cells to place the solution containing the unadsorbed dye into the UV-VIS device to measure the remaining dye concentration. The measurement process was carried out at a wavelength of 495 nm (Fig, 2).

3. Result and Discussion

3.1. FTIR spectra

FTIR spectra of (Zn_2BO_3) obtained are shown in (Fig.3). The peak at 3387.11 cm^{-1} is due to O–H groups in zinc borate [17]. The peak at 1508.38 cm^{-1} and the peak at 1388.79 cm^{-1} belong to the asymmetric stretching of B (3)–O and in-plane bending of B–O–H, respectively. The peaks at 1041.6 and 837.31 cm^{-1} are for asymmetric and symmetric stretching vibrations of B (4)–O, respectively. The peak at 551.66 cm^{-1} is attributed to the in-plane bending of B (3)–O. The peak at 470 cm^{-1} is due to the bending of Zn–O.

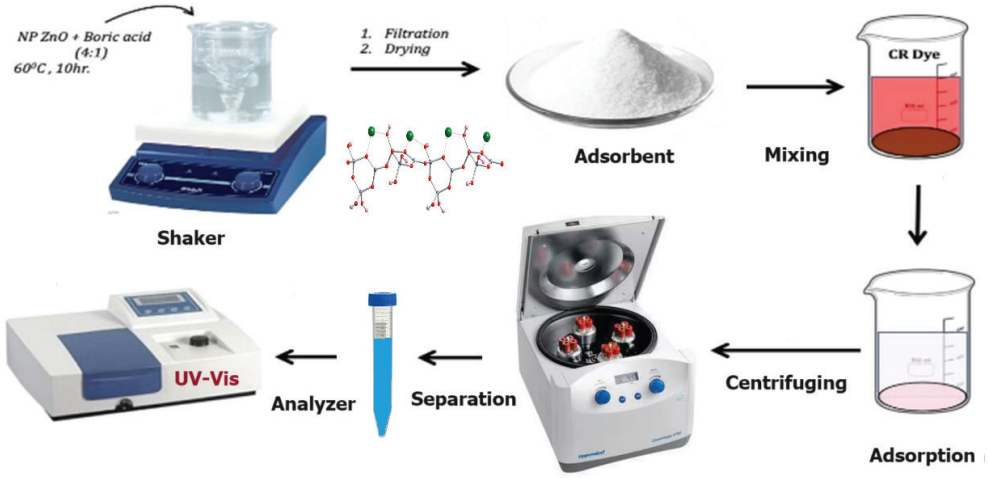

Fig. 2. Schematic diagram of the adsorption process with Zn_2BO_3

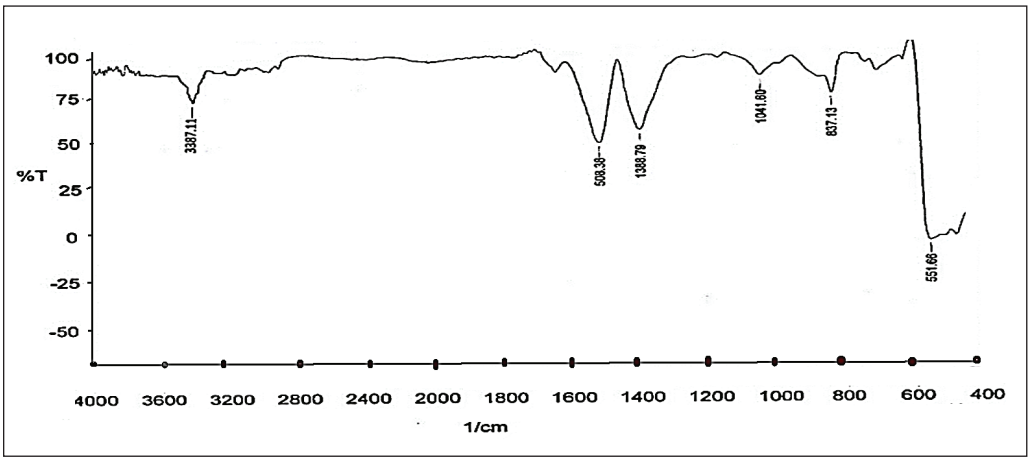

Fig. 3. FTIR spectra of Zn_2BO_3

3.2. XRD analysis

XRD pattern of (Zn_2BO_3) shown in Figure 4 values of (2θ) for the main peaks of zinc borate were reported as 19.0°, 21.03°, 23.0°,25.11°, 29.0°,31.22°,32.16° and 37.0° [18]. It is completely consistent with the XRD pattern explained in the literature [19].

3.3. SEM analysis

The shapes represent images of the scanning electron microscope with a field of light emission of the prepared compound, the figures of the compound showed semi-spherical shapes as well as an image that took the presence of a conglomerate in the prepared compound and that the surface of the compound contains holes and pores [20], and that the presence of these pores increases the surface area of the compound and therefore these holes will play an important role in increasing adsorption as shown in Figure 5a-f that crystals of the compound fall within the nanoscales of Zn_2BO_3.

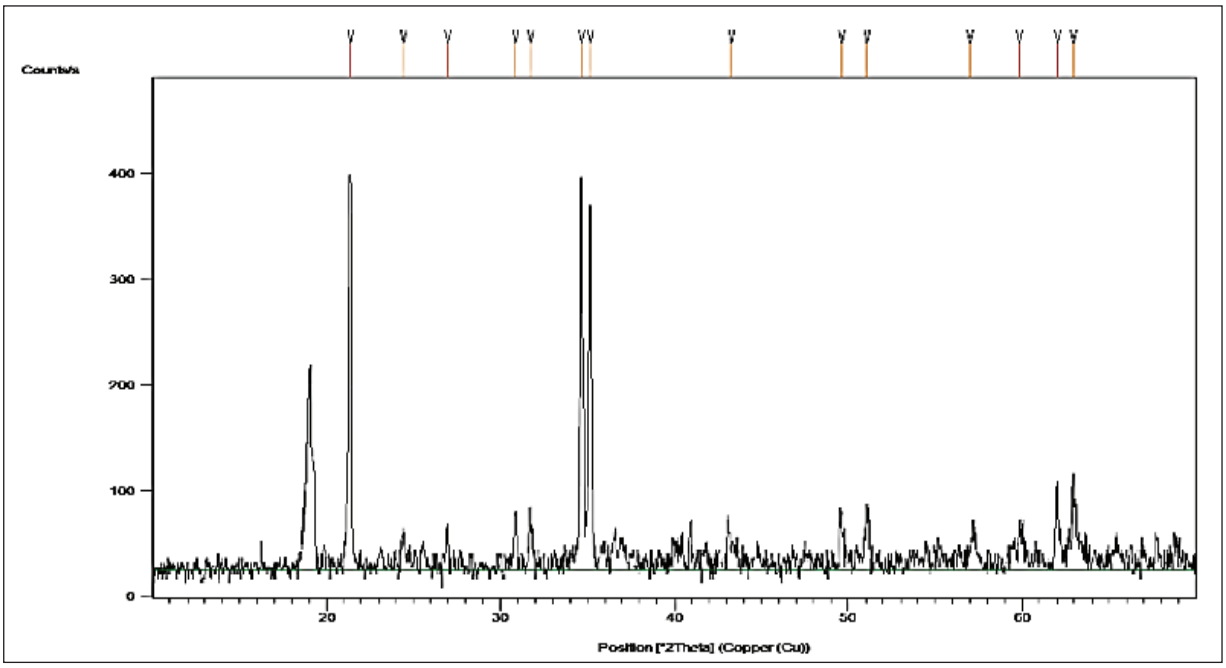

Fig.4. XRD Patterns of Zn_2BO_3

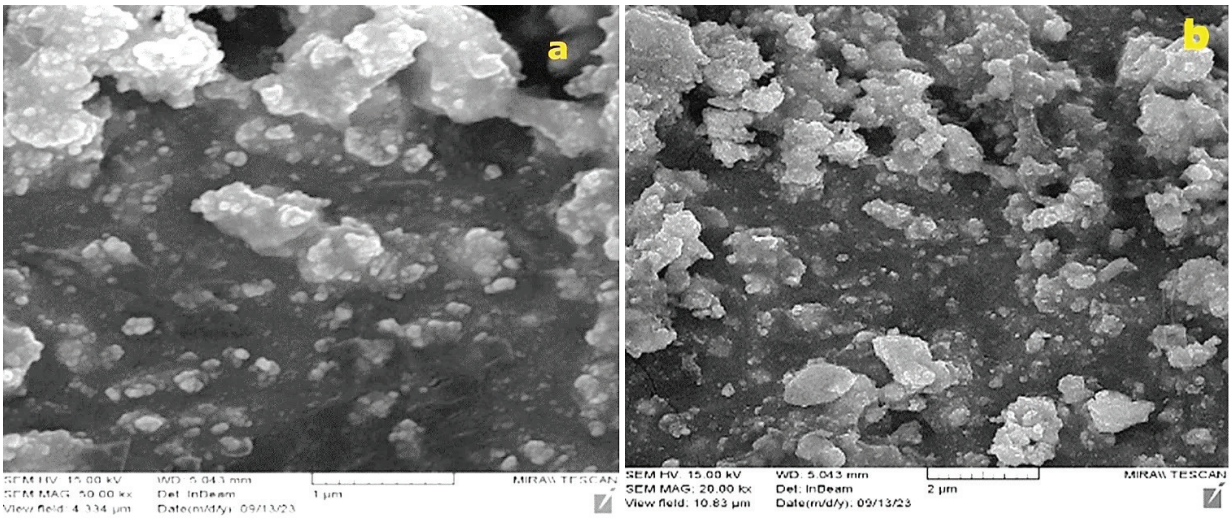

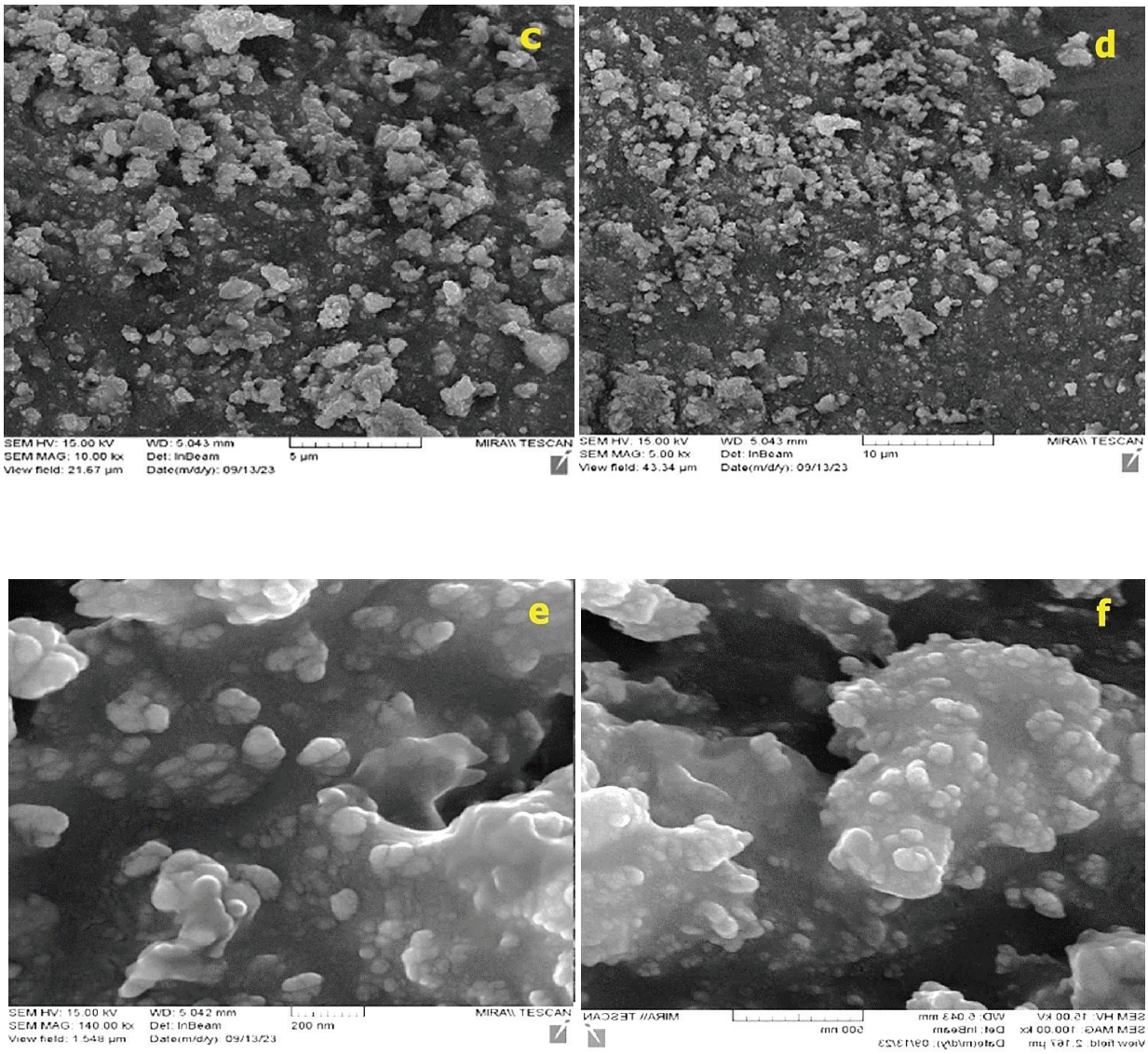

Fig. 5a-f. SEM of nanoscales of Zn_2BO_3

3.4. EDX analysis

EDX analysis of Zn_2BO_3 is shown in Table 1 and Figure 6. The theoretical composition of zinc borate is 63.31% zinc, 30.97% oxygen, and 5.23%. The chemical composition of the (Zn_2BO_3) sample was determined as 65.67% zinc, 29.01% oxygen, and 5.32% boron by data EDX analysis. While the experimental and theoretical composition values of Zn and O are near each other, the value of B is completely different as the boron element has low atomic mass [21].

3.5. Zeta Potential Analysis

There are many different ways of calculating zeta potential. In this study, the method of calculating zeta potential is electrophoretic (Table 2).

As shown in Figure 7 and Table 3, the value of the zeta potential of zinc borate (-36.0 mv) means the surface of the product has a negative charge, it is stable [22], and it is good to use to adsorb CR from aqueous solution. Zinc borate product is too difficult to make colloid with a solution so it was easy to isolate it from an aqueous solution to measure the amount of adsorption.

Table 1. EDX values of Zn_2BO_3 composition.

Composition	W %	A %
B	5.32	14.87
O	29.01	54.78
Zn	65.67	30.35
Total	100.00	100.00

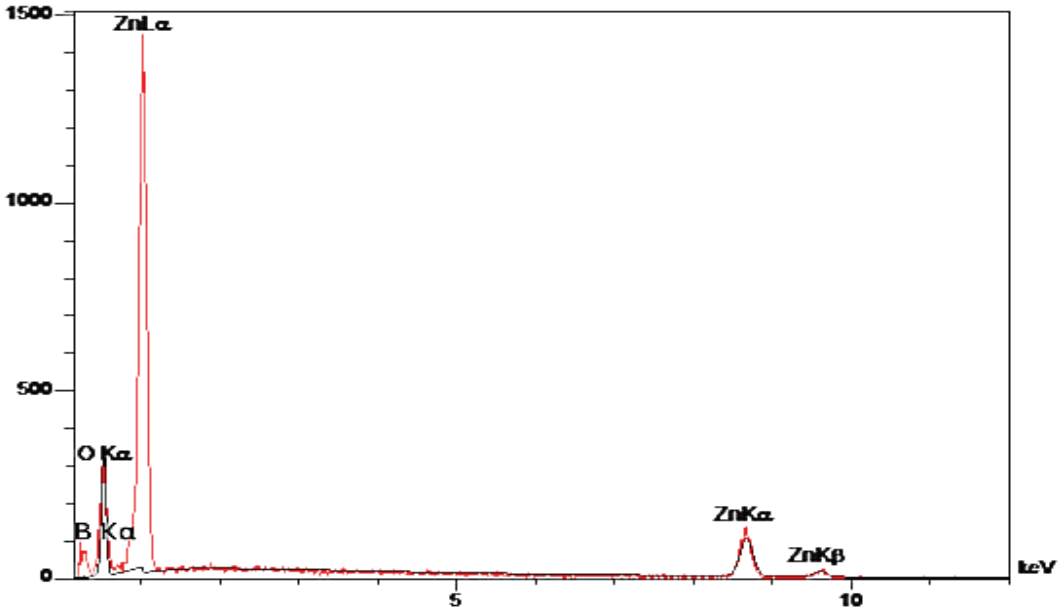

Fig. 6. The EDX positions of the (Zn_2BO_3) compound

Table 2. The range of stability according to Zeta potential analysis

Stability behavior of the particles	Zeta Potential (mV)
Rapid Coagulation or Flocculation	0 to ±5
Incipient Instability	±10 to ±30
Moderate Stability	±30 to ±40
Good Stability	±40 to ±60
Excellent Stability	More than ±61

Table 3. The zeta potential of Zn_2BO_3

Peak NO:	zeta potential	Electrophoretic
1	-36.0 mV	- 0.000186

3.6. Determination of the calibration curve

The calibration curve of the dye was calculated by preparing different concentrations of 5,10,15,20,25 mg L^{-1} at pH = 8 and the absorption was measured at the highest wavelength 495 nm by plotting concentration versus absorption, where $R^2 = 0.9973$ represents the linear equation as in Figure 8

3.7. Adsorption Studies

3.7.1.Study of equilibrium time

The factor affecting adsorption efficiency is the equilibrium time between the adsorbent (Zn_2BO_3) and CR dye [23]. The equilibrium time for adsorption of CR dye by 0.1 g of Zn_2BO_3 adsorbent was studied between 1-100 min in a dye

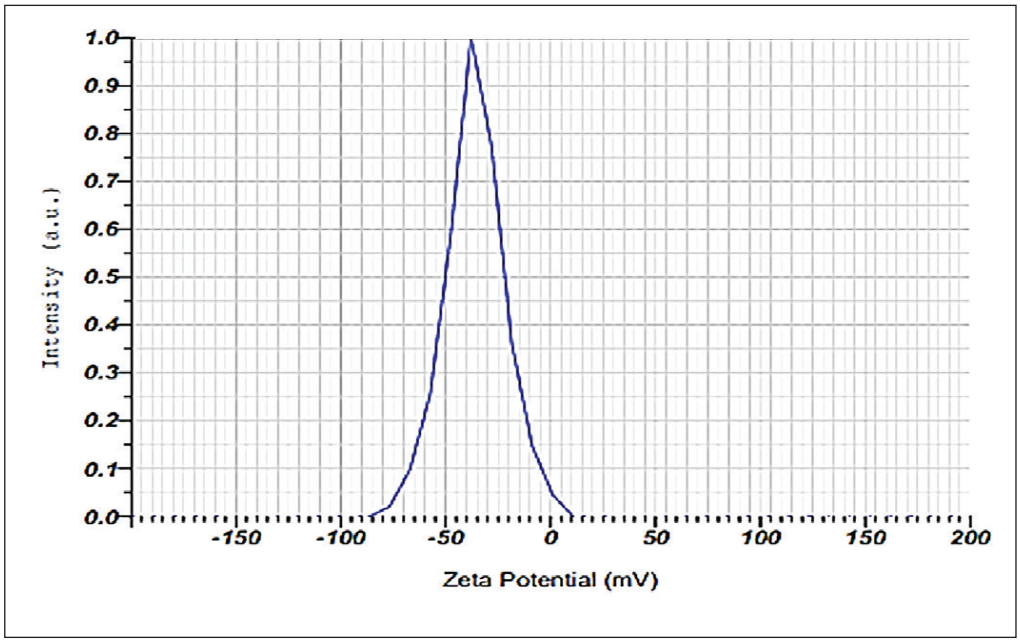

Fig.7. Zeta potential position of Zn_2BO_3 surface

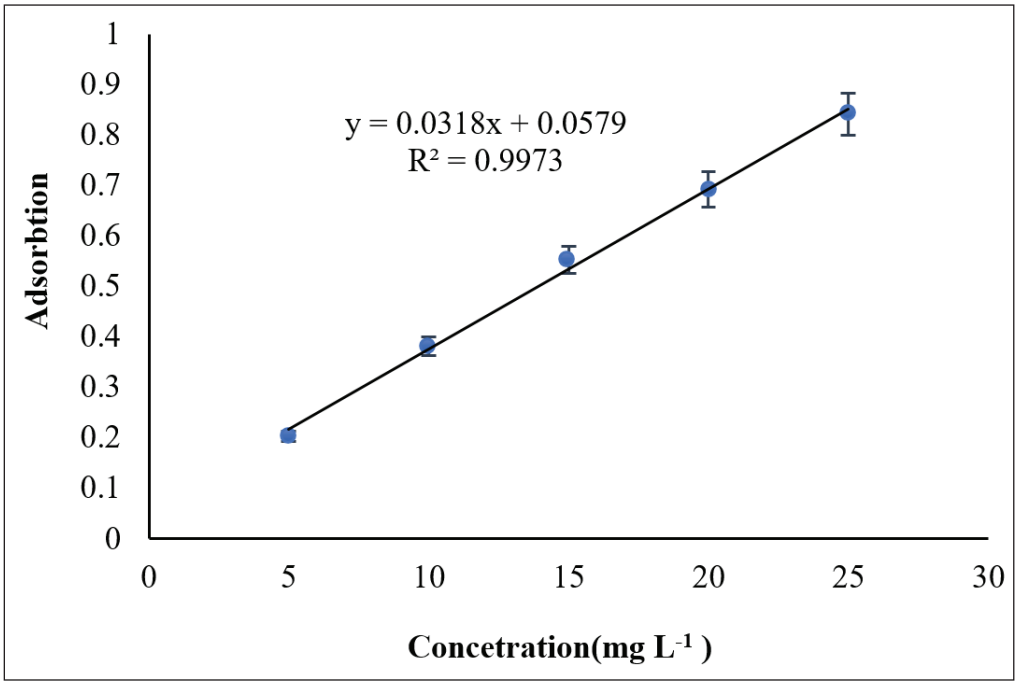

Fig. 8. The calibration curve of CR dye at pH 8

Table 4. Equilibrium time of adsorption Cr dye on Zn_2BO_3 adsorbent

Time (min)	5	10	15	30	45	60
q (mg g^{-1})	9.61949	13.2673	16.411	17.355	17.4811	17.669

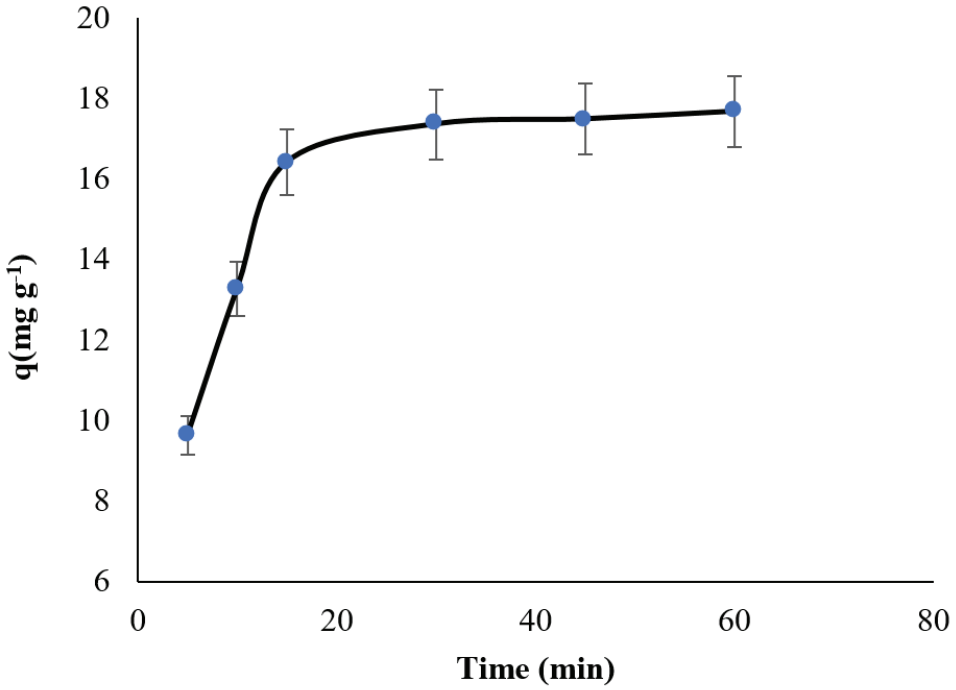

Fig. 9. The effect of time on adsorption of CR dye by Zn_2BO_3 adsorbent

concentration of 25 mg L^{-1} and 300 K^0. According to Figure 9 and Table 4, The equilibrium time of 30 minutes is the best time for the adsorption process. The absorption capacity was obtained at 17.355. The amount of adsorbate on Zn_2BO_3 adsorbent (qe =mg g^{-1}) is calculated by Equation 1.

$$q = \frac{(C_o - C_e)V}{M} \qquad \text{(Eq.1)}$$

C_0: initial concentration of CR in solution
C_e: Remaining concentration of CR in solution
V: Volume of solution
M: Wight of adsorbent ZB

3.7.2. Optimization parameters

Due to previous research main parameters such as adsorbent amount, pH, effect of initial concentration, the effect of temperature, sample volume, and capacity absorption for the extraction or removal of various organic materials based on different nanoparticle adsorbents (carbon nanotube, bismuth oxide nanoparticles) must be analyzed [24-26].

3.7.2.1. Effect of adsorbent amount

The effect of altering the adsorbent amount on the CR dye adsorption was studied using different amounts of Zn_2BO_3 adsorbent (0.1,0.0.2,0.03,0.06 g) in 60 min, the dye concentration of 25 mg L^{-1}, and sample volume of 100 mL at wavelength 495 nm. It was found that the adsorption of CR dye was increased by increasing catalyst weight due to the high surface area and active sites [27] as shown in Table 5 and Figure 10.

Table 5. amount of CR dye adsorbed on (Zn_2BO_3) adsorbent in (mg g^{-1})

Amount of ZB (g)	0.06	0.1	0.2	0.3
$q_{(mg/g)}$	2.261	6.034	8.77	11.82

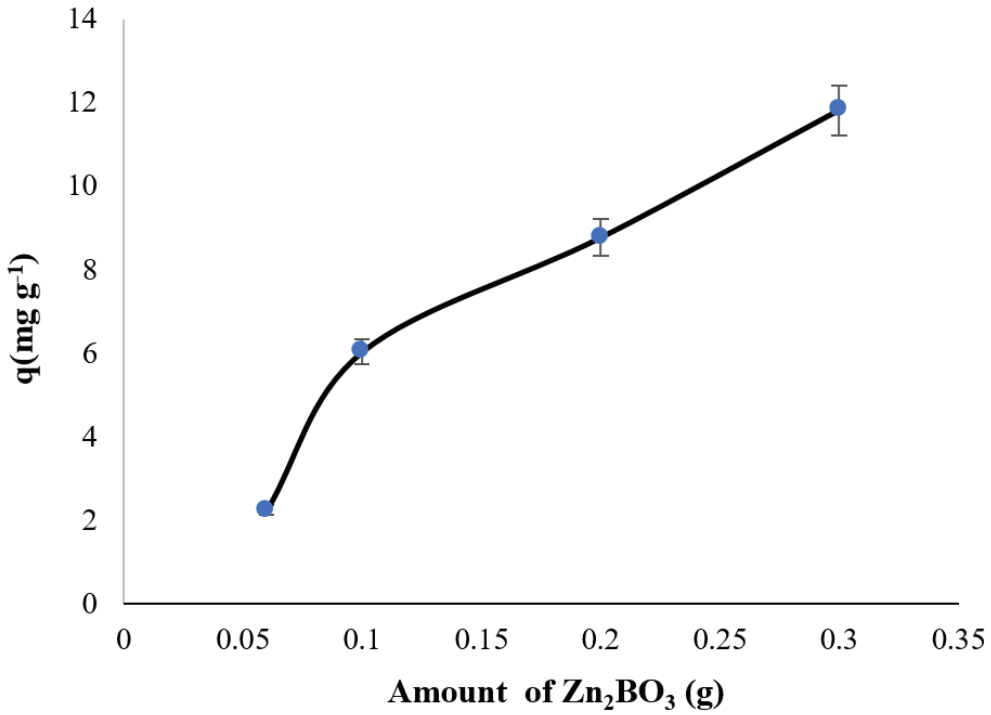

Fig. 10. The effect of the amount of Zn_2BO_3 adsorbent on the adsorption of CR dye

3.7.2.2. Effect of pH

The removal efficiency of CR dye using 0.1 g of Zn_2BO_3, 100 mL of sample, and 25 mg L^{-1} CR dye was evaluated in different pH (3,5,7,9,11) at 60 min. The adsorption of the dye in an acidic medium is greater than in a base medium as shown in Table 6 and Figure 11. It is related to the ability of dye tendency to bind in an acidic medium with the catalyst more than its tendency to bind with solvent molecules. The removal processing of dye by photocatalysis is subject to several mechanisms, including direct reduction by electrons in the conduction beam, direct oxidation through gaps in the valence beam, and finally, hydroxy radical attack [28]. These mechanisms mentioned depend on the nature of the material and the pH function of the medium in which the adsorption process takes place has an effect on both adsorbate and adsorbent. However, it should be noted that this dye is deposited at pH=2 and also changes the color of dye at acid function pH=3 causing a difference in wavelength, so it was settled to use the pH = 5.5 in the next experiments.

Table 6. Effect pH on adsorption amount of CR dye on (Zn_2BO_3) adsorbent.

pH	3	5	7	9	11
Adsorbate (q)	24.525	20.154	9.933	17.292	17.732

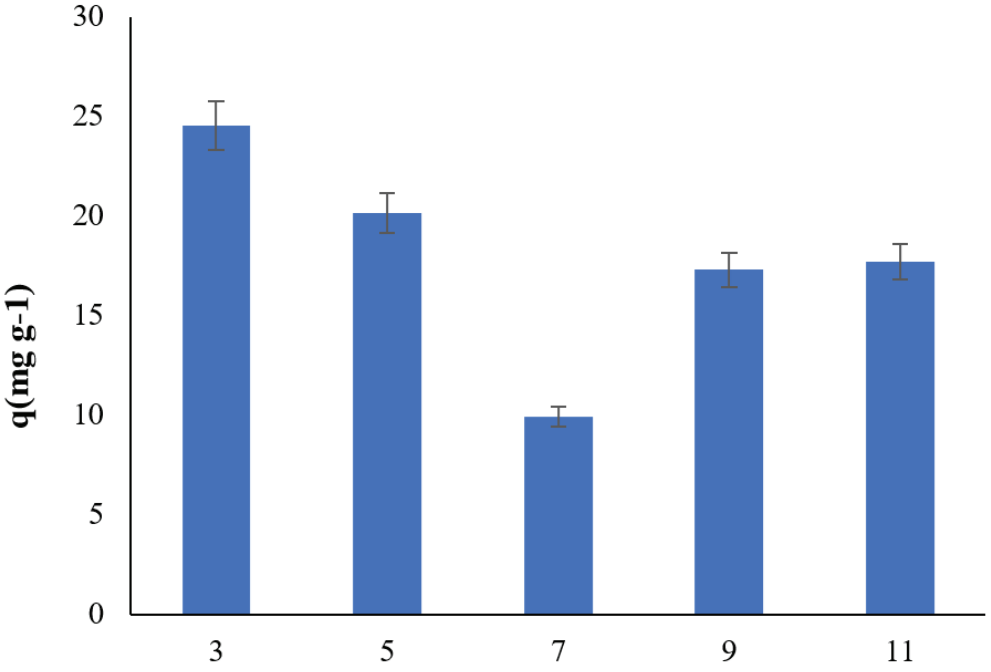

Fig. 11. The effect of pH solution on adsorption of CR dye

3.7.2.3. Effect of initial dye concentration

The dye concentration affects the adsorption process. So, in this study, different concentrations of red Congo dye were taken. At values of 50,75,100,125,150 mg L^{-1} with a constant amount of adsorbent of zinc borate, the adsorption efficiency was increased by increasing concentrations of dye where the highest adsorption value was recorded [29] as shown in Table 7 and Figure 12. This is because the largest amount of dye will be adsorbed on the adsorbent and the generation of free radicals for hydroxyl will decrease due to a lack of active sites of hydroxyl ions. The percentage of adsorption in high initial concentration of dye did not increase which hinders access of photons of light to the catalytic surface causing a decrease in absorption of photons and, consequently a decrease in decomposition rate. The maximum adsorption capacity of Zn_2BO_3 was obtained at 61.028 mg g^{-1} for 150 mg L^{-1} of CR dye.

Table 7. The effect of initial dye concentration on the adsorption amount of CR dye by Zn_2BO_3

C_0	50 mg L^{-1}	75 mg L^{-1}	100 mg L^{-1}	125 mg L^{-1}	150 mg L^{-1}
q (mg g^{-1})	35.556	48.026	48.292	54.896	61.028

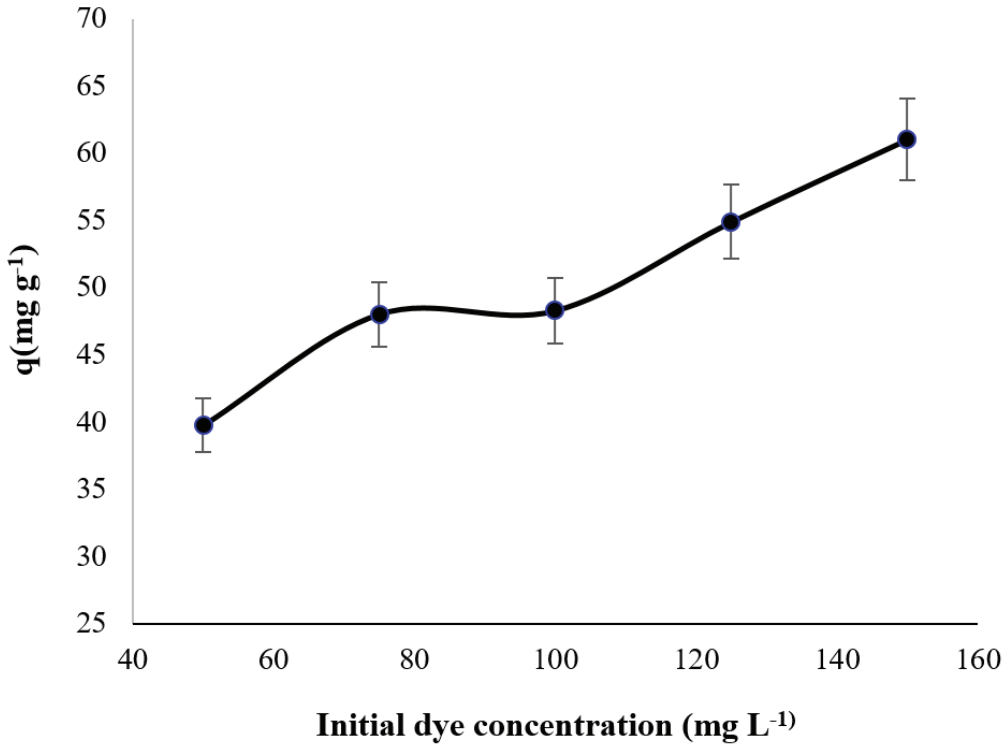

Fig. 12. The effect of initial dye concentration on adsorption of CR dye

3.7.2.4. Effect of Temperature

The temperature of the medium that occurs when adsorption is one of the factors affecting dye removal. In this study, the measurements were made within three temperatures (300^0K,318^0K,333^0K) where it was found that the efficiency of adsorption increases with increasing temperature degrees and accelerates access to equilibrium time [30], where the measurements made at a constant concentration and different times extended from (5-90 min). Also, the amount of adsorbent Zn_2BO_3 used to adsorb CR dye was 0.1 g and the adsorption efficiency increased due to obstruction of rearrangement electron-gap process. Due to increased temperature, this cycle proves that the adsorption process on this adsorbent is endothermic. In addition, the high temperature increases the oxidation rate of organic compounds and thus enhances decomposition capacity (Table 8 and Fig. 13).

Table 8. Effect of temperature on adsorption amount of CR dye on Zn_2BO_3 adsorbent in (mg g^{-1}).

Time(min)	300 K		318K		333K	
Zn_2BO_3	C_e	q	C_e	q	C_e	q
5	24.37	25.62	18.02	31.97	12.70	37.29
10	20.56	29.43	16.16	33.83	8.336	41.66
15	11.38	38.61	7.990	42.00	5.349	44.65
30	9.216	41.78	7.361	42.63	4.279	45.62
45	7.518	42.48	6.921	43.07	4.185	45.81
60	7.330	42.73	6.229	43.77	3.965	46.03

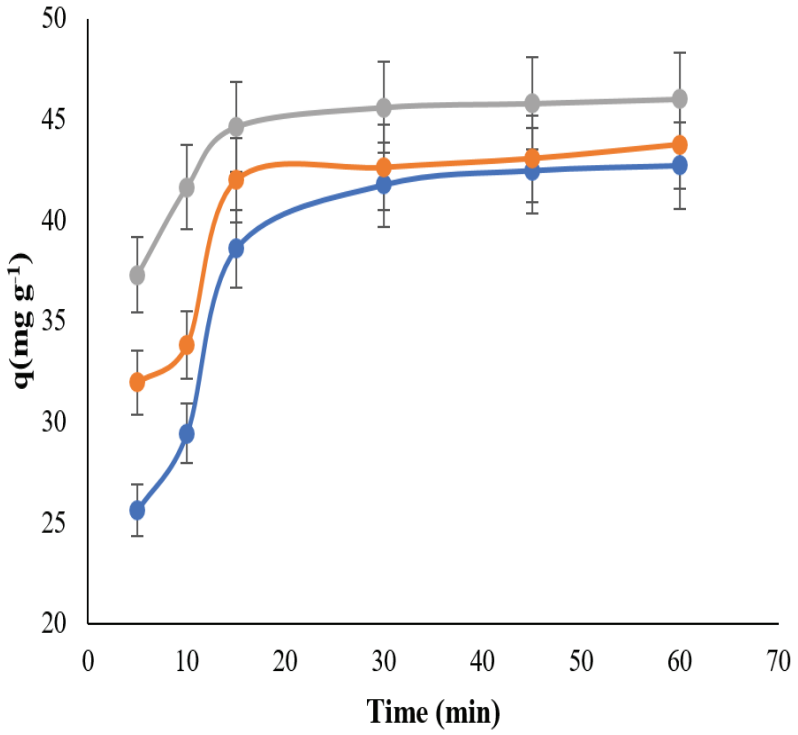

Fig. 13. The effect of temperature on adsorption of CR dye, blue line (300oK), orange line (318oK), and gray line (333oK)

3.8. Adsorption Isotherm

Calculations and study of adsorption isotherm, calculations of effect primary dye concentration at room temperature 300^{0}K was used to apply the mathematical equation of isotherm Langmuir by plotting linear equation of Langmuir equation based on values of C_e and C_e/q_e as shown in Table 9. and Figure 14. Langmuir constant (K_L=0.0525), values of maximum adsorption (Q_{max}=212.7), and correlation coefficient (R^2=98) were obtained for Zn_2BO_3. The linear relationship of the Freundlich equation based on values of log Ce versus log qe is shown in Table 10 and Figure 15. The Freundlich constants such as T=300^{o}K, R^2=0.8993, n=3.86, and Kf=3.556 were calculated. The R^2 value of Langmuir and Freundlich isotherm is 0.98 and 0.8993, respectively. So, the adsorption process flows by Langmeyer's isotherm model.

Table 9. Langmeyer isotherm study for adsorption amount of CR dye (mg g^{-1}).

C_0 (mg L^{-1})	C_e	q_e	C_e/q_e
50	14.443	35.556	0.1354
75	26.973	48.026	0.2246
100	51.707	48.292	0.3569
125	70.103	54.896	0.4256
150	88.971	61.028	0.4859

Table 10. Freundlich's adsorption Isotherm for adsorption amount of CR dye (mg g-1).

C_0	50	75	100	125	150
Log C_e	1.1596	1.4309	1.7135	1.8457	1.9492
Log q_e	1.9492	1.6814	1.7838	1.7395	1.7855

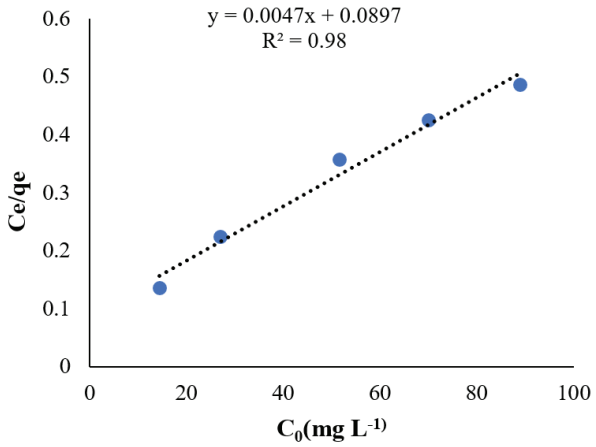

Fig. 14. Langmeyer adsorption Isotherm

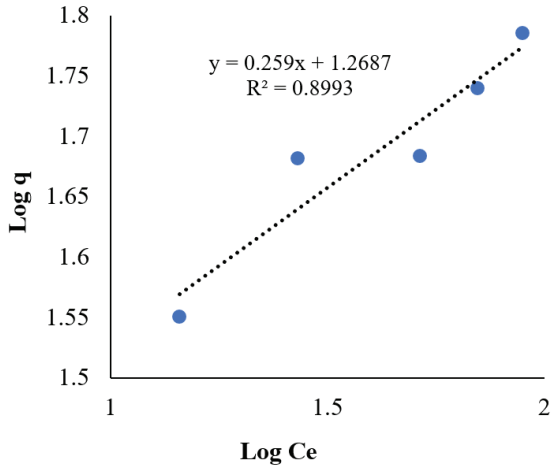

Fig. 15. Freundlich adsorption Isotherm

3.9. Thermodynamic study

Due to the temperature effect, the thermodynamic functions (ΔH enthalpy, ΔG free energy, and ΔS entropy) were calculated. For the adsorption of red Congo dye on adsorbent (Zn_2BO_3) the importance of these functions to understanding the adsorption process. Table 11 represents values of both ln k_c and values of temperature, while Figure 16 shows a relationship between ln K_c versus the inverse of time (1/T), from which the values of (ΔH, (ΔS) can be obtained that can be calculated through values of interception= (ΔH/R) and slop= (ΔS/R). Table 12 shows thermodynamic values.

Table 11. values of both (ln k_c) and values of Inverse temperature

T(K^0)	300	318	333
1/T * 10^{-3}	3.333	3.144	3.003
Ln K_c	1.5	1.66	2.122

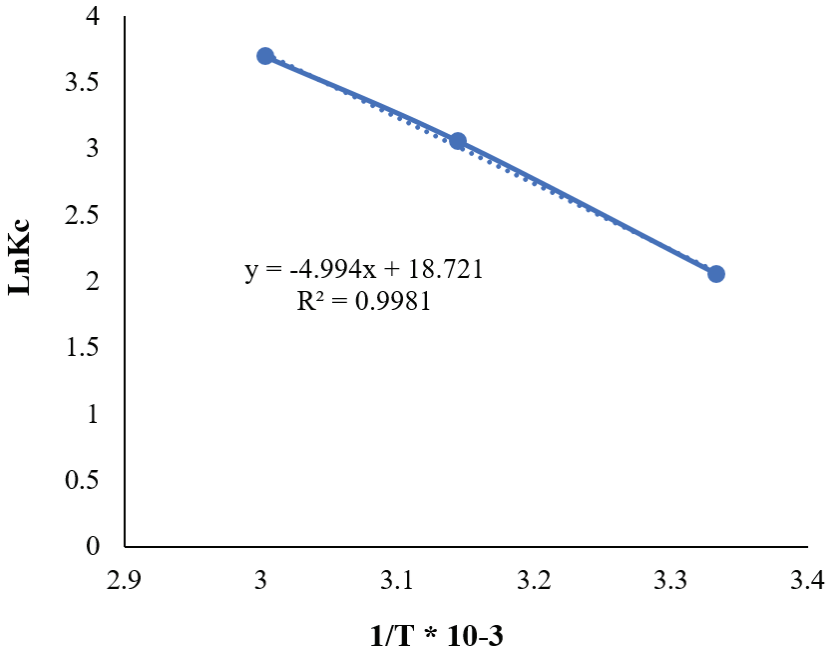

Fig. 16. Linear relationship between lnk_c vs. $1/T*10^{-3}$

Table 12. values of (ΔH enthalpy, ΔG free energy, ΔS entropy)

Compound	ΔG(KJ mol^{-1})			ΔS(KJ K^{-1} mol^{-1})	ΔH(KJ mol^{-1})
	300 K^0	318 K^0	333 K^0		
ZB	-(3.741)	-(4.388)	-(5.875)	62.65	15.2

From the values shown above in Table 13. we conclude, free energy value ΔG of adsorption all negative, which is evidence that adsorption process is spontaneous. Entropy value ΔS for the adsorption of CR dye on adsorbent (Zn_2BO_3) is positive, indicating that adsorbent molecules are in continuous motion on the surface of the adsorbent, causing an increase in system randomness. The value of adsorption temperature enthalpy ΔH is positive for adsorption indicating that the adsorption process is endothermic and that increased temperature leads to the increased rate of propagation speed of adsorbed particles on the adsorbent surface between pores in the adsorbent surface. The pseudo-first-order equation is called Lagergren, where experimental data is applied. The pseudo-second-order equation shows that the adsorption rate depends on the adsorption amplitude in the adsorption surface, (Lagergren Pseudo second order – equation).

Table 13. values of (ln qe-qt) versus the time values of the adsorption process

Time	5	10	15	30	45	60
q_e	42.7327	42.7327	42.7327	42.7327	42.7327	42.7327
q_t	34.619	38.267	41.411	42.353	42.481	42.732
$\ln(q_e-q_t)$	2.093	1.496	0.278	-0.974	-1.38	NUM

Table 13 shows the value of ln qe-qt and time values (t) of the adsorption process of CR on adsorbent Zn_2BO_3 and Figure 17 represents the linear relationship of the false first-order equation, from which the adsorption rate constant (K_1), the adsorption capacity (q_e) and the correlation coefficient shown in Table 14 were calculated. Values in Table 14 it clear that the process of adsorption of red Congo dye on Zn_2BO_3 adsorbent follows the second kinetic equation for the reasons, the large difference between values of adsorption capacity calculated according to the false first order equation qe(cal) is different from the experimental adsorption value qe(exp) obtained through this study. As shown in Figure 17, the linear axis of the false first-order equation does not pass through all points, unlike the linear axis of the false second-order equation, which passes exactly all points as shown in Figure 18. The correlation value R^2 of the false first-order equation is less than 0.8986 away from the value of 1, unlike the correlation value of R^2 of the false second-order equation, which is limited to 0.999.

4. Conclusion

Zinc Borate is successfully synthesized by one-step precipitation from nano zinc oxide and Boric acid. The absorption of CR Day based on Zn_2BO_3 adsorbent was determined by UV-Vis spectroscopy. FTIR spectra showed the position of active aggregates of the compound. It clearly showed their importance in the process of dye adsorption. XRD analysis position of 2Θ for crystal lattice patterns proved the formation of the desired compound and clarified the dimensions and size of the crystal. SEM analysis images of compound surface contain holes and pores, EDX analysis explained compassion component. Zeta potential analyses indicate (Zn_2BO_3) has a negative charge, and it is stable. All effective factors in the adsorption process have been studied and isotherm and kinetic have been explained.

Table 14. Adsorption capacity (qe) and the correlation coefficient of false first-order equation

Equation	Comp	$Q_{e,exp}$	$K_1(min^{-1})$	$q_e(mg\ g^{-1})$	R^2
False first-order equation	ZB	42.732	0.00146	8.483	0.8986
False second-order equation	ZB	42.732	0.20092	43.66	0.999

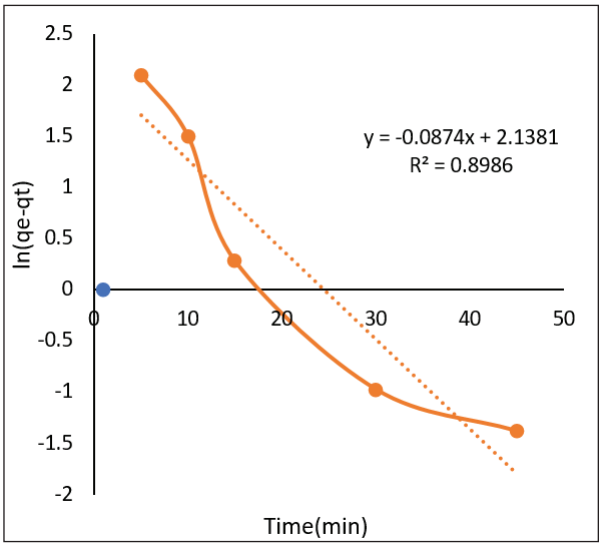

Fig. 17. Linear relationship of the first-order

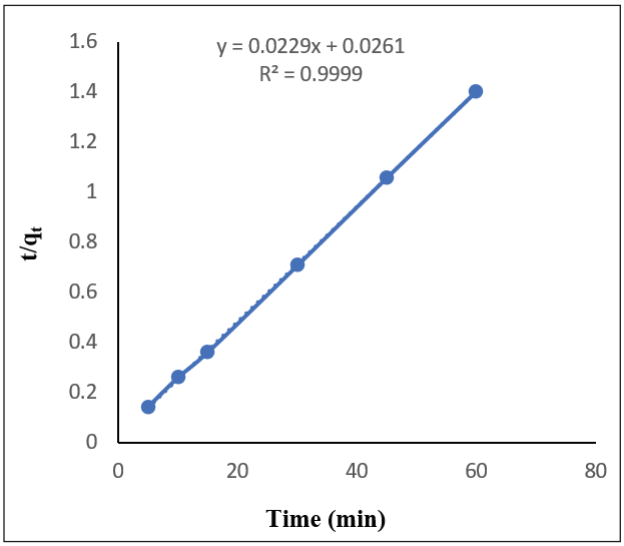

Fig. 18. L linear relationship of the second-order

5. References

[1] K. Shen, S. Kochesfahani, F. Jouffret, Zinc borates as multifunctional polymer additives, Polymer Adv. Technol., 19 (2008) 469-474. https://doi.org/10.1002/pat.1119

[2] D. M. Schubert, Hydrated zinc borates and their industrial use, Molecules, 24 (2019) 2419. https://doi.org/10.3390/molecules24132419

[3] M. Yusuf, S. Mohd, M. Faqeer, Natural colorants: Historical, processing and sustainable prospects, Nat. Prod. Bioprospect., 7 (2017) 123-145. https://doi.org/10.1007/s13659-017-0119-9

[4] A.K. Roy Choudhury, (2014). Environmental impacts of the textile industry and its assessment through life cycle assessment. In: Muthu, S. (eds) Roadmap to sustainable textiles and clothing. Textile Sci. Cloth. Technol., Springer, Singapore, 2014. https://doi.org/10.1007/978-981-287-110-7_1

[5] N. Akhtar, M.I Syakir Ishak, S.A. Bhawani, K. Umar, Various natural and anthropogenic factors responsible for water quality degradation, A review, Water, 13 (2021) 2660. https://doi.org/10.3390/w13192660

[6] M. Smail, K. Akhtar, M.I. Khan, T. Kamal, M.A. Khan, A. M Asiri, S.B. Khan, Pollution, toxicity, and carcinogenicity of organic dyes and their catalytic bio-remediation, Curr. Pharm. Des., 25 (2019) 3645-3663. https: // doi.org/10.2174/1381612825666191021142026

[7] R. Ashouri, Dynamic and static removal of benzene from air based on task-specific ionic liquid coated on MWCNTs by sorbent tube-headspace solid-phase extraction procedure, Int. J. Environ. Sci. Technol., 18 (2021) 2377-2390. https://doi.org/10.1007/s13762-020-02995-4

[8] M.M. Asl, Functionalized graphene oxide with bismuth and titanium oxide nanoparticles for efficiently removing formaldehyde from the air by photocatalytic degradation–adsorption process, J. Anal. Test., 7 (2023) 444-458. https://doi.org/10.1007/s41664-023-00272-0

[9] A. Faghihi-Zarandi, New method for removal of hazardous toluene vapor from air based on ionic liquid-phase adsorbent, Int. J. Environ. Sci. Technol., 16 (2019) 2797–2808. https://doi.org/10.1007/s13762-018-1975-5

[10] S. Teimoori, A.H. Hassani, M. Panahi, An immobilization of aminopropyl trimethoxysilane-phenanthrene carbaldehyde on graphene oxide for toluene extraction and separation in water samples, Chemosphere, 316 (2023) 137800. https://doi.org/10.1016/j.chemosphere.2023.137800

[11] M. Abadi, Air pollution control: The evaluation of TerphApm@ MWCNTs as a novel heterogeneous sorbent for benzene removal from air by solid phase gas extraction, Arab. J. Chem., 13 (2020) 1741-1751. https://doi.org/10.1016/j.arabjc.2018.01.011

[12] J. Rakhtshah, A rapid extraction of toxic styrene from water and wastewater samples based on hydroxyethyl methylimidazolium tetrafluoroborate immobilized on MWCNTs by ultra-assisted dispersive cyclic conjugation-micro-solid phase extraction, Microchem. J., 170 (2021) 106759. https://doi.org/10.1016/j.microc.2021.106759

[13] R. Liang, A. Hu, Robert, M. Hatat-Fraile, N. Zhou, Fundamentals on adsorption, membrane filtration, and advanced oxidation processes for water treatment, Nanotechnol. Water Treat. Purif., (2014) 1-45. https: /doi.org/10.1007/978-3-319-06578-6_1

[14] W. Liu, A. Tkatchenko, M. Scheffler, Modeling adsorption and reactions of organic molecules at metal surfaces, Acc. Chem. Res., 47 (2014) 3369-3377. https://doi.org/10.1021/ar500118y

[15] T.U.T Dao, H.T.T, D.T.C Nguyen, H.T. LE, H.T. Nguyen, S.T. Do, T.D Nguyen, Process optimization studies of Congo red dye adsorption onto nickel-iron layered double hydroxide using response surface methodology, Solid State Phenomena, 298 (2019) 83-88. https://doi.org/10.4028/www.scientific.net/SSP.298.83

[16] A. Yalçın, G. Mehmet, A novel approach for the production of zinc borate ($4ZnO{\cdot}B_2O_3{\cdot}H_2O$) using a single-step hydrothermal method, Main Group Met. Chem., 44 (2021) 1-8. https://doi.org/10.1515/mgmc-2021-0001

[17] Y.Y. Zhang, L. Ping, H.L. Zhi, Controllable synthesis and flame-retardant properties of bunch-, chrysanthemum-, and plumy-like $4ZnO{\cdot}B_2O_3{\cdot}H_2O$ nanostructures, Powder Technol., 210 (2011) 208-211. https://doi.org/10.1016/j.powtec.2011.03.018

[18] R. Stefan, P. Pascuta, A. Popa, O. Raita, E. Indera, E. Culea, XRD and EPR structural investigation of some zinc borate glasses doped with iron Ions, J. Phys. Chem. Solids, 73 (2012) 221-226. https://doi.org/10.1016/j.jpcs.2011.10.039

[19] X. Shi, M. Li, PEG-300 assisted hydrothermal synthesis of $4ZnO{\cdot}B_2O_3{\cdot}H_2O$ Nanorods, Materials Research Bulletin 42.9 (2007) 1649-1656. https://doi.org/10.1016/j.materresbull.2006.11.034

[20] M. Vayer, C. Serré, N. Boyard, C. Sinturel, R. Errer, Surface morphologies of composites based on unsaturated polyester pre-polymer, J. Mater. Sci. 37 (2002) 2043-2051. https://doi.org/10.1023/A:1015263618720

[21] C. Zhao, Y. Jiao, Y. K. Chen, G. Ren, The tribological properties of zinc borate ultrafine powder as a lubricant additive in sunflower oil, Tribol. Trans., 57 (2014) 425-434. https://doi.org/10.1080/10402004.2013.878776

[22] I. Mohammed, D. Al Shehri, M. Mahmoud, M. S. Kamal, O. S. Alade, A surface charge approach to investigating the influence of oil contacting clay minerals on wettability alteration, ACS Omega, 6 (2021) 12841-12852. https://doi.org/10.1021/acsomega.1c01221

[23] R. Labied, O. Benturki, A. Y. Eddine Hamitouche, A. Donnot, Adsorption of hexavalent chromium by activated carbon obtained from a waste lignocellulosic material (Ziziphus jujuba cores): Kinetic, equilibrium, and thermodynamic study, Adsorp. Sci. Technol., 36 (2018) 1066-1099. https://doi.org/10.1177/0263617417750739

[24] S. Teimoori, New extraction of toluene from water samples based on nano-carbon structure before determination by gas chromatography, Int. J. Environ. Sci. Technol., 20 (2023) 6589-6608. https://doi.org/10.1007/s13762-023-04906-9

[25] S. Teimoori, Rapid extraction of BTEX in water and milk samples based on functionalized multi-walled carbon nanotubes by dispersive homogenized-micro-solid phase extraction, Food Chem., 421 (2023) 136229. https://doi.org/10.1016/j.foodchem.2023.136229

[26] A. Faghihi-Zarandi, J. Rakhtshah, BB. Yarahmadi, A rapid removal of xylene vapor from environmental air based on bismuth oxide coupled to heterogeneous graphene/graphene oxide by UV photo-catalectic degradation-adsorption procedure, J. Environ. Chem. Eng., 8 (2020) 104193. https://doi.org/10.1016/j.jece.2020.104193

[27] G. Leofanti, M. Padovan, G. Tozzola, B. J. C. T. Venturelli, Surface area and pore texture of catalysts, Catal. Today, 41 (1998) 207-219. https://doi.org/10.1016/S0920-5861(98)00050-9

[28] B.K. Hashim, N. K. Zaki, Preparation and study photocatalytic properties of BiOX (X= Cl, Br, I), J. Kufa Chem. Sci., 2 (2022) 50-68. https://journal.uokufa.edu.iq/index.php/jkcs/article/view/11089

[29] C.H. Wu, Comparison of azo dye degradation efficiency using UV/single semiconductor and UV/coupled semiconductor systems, Chemosphere, 57 (2004) 601-608. https://doi.org/10.1016/j.chemosphere.2004.07.008

[30] L. Karimi, S. Zohoori, E.Y. Mohammad, Photocatalytic degradation of azo dyes in aqueous solutions under UV irradiation using nano-strontium titanate as the nano photocatalyst, J. Saudi Chem. Soc., 18 (2014) 581-588. https://doi.org/10.1016/j.jscs.2011.11.010